Proc. Natl. Acad. Sci. USA
Vol. 84, pp. 1585–1589, March 1987
Cell Biology

Simultaneous electrical and optical measurements show that membrane fusion precedes secretory granule swelling during exocytosis of beige mouse mast cells

(capacitance measurements/video microscopy/GTP/osmotic/vesicle)

JOSHUA ZIMMERBERG*, MICHAEL CURRAN*†, FREDRIC S. COHEN‡, AND MALCOLM BRODWICK†

*Physical Sciences Laboratory, Division of Computer Research and Technology, and *Molecular Forces and Assembly Section, Laboratory of Biochemistry and Metabolism, National Institutes of Health, Bethesda, MD 20892; †Department of Biophysics and Physiology, University of Texas Medical Branch, Galveston, TX 77550; and ‡Department of Physiology, Rush Medical College, Chicago, IL 60612

Communicated by DeWitt Stetten, Jr., November 19, 1986

ABSTRACT **Mast cells show dramatic morphological changes when undergoing exocytosis. We have investigated whether the first of those morphological changes, swelling of the secretory granule, precedes—and therefore possibly initiates—secretion or whether it occurs after fusion of the granule and plasma membranes. We used cell membrane capacitance to detect the moment when granule and plasma membrane become continuous. We measured large capacitance increases, often preceded by transients in capacitance. The rise-times of the capacitance increases were half-maximal at 2–59 msec. We observed cells with high-resolution video microscopy while these measurements were done. The capacitance increase always preceded the granular swelling that leads to exocytosis. To rule out the possibility that fusion was induced by a mechanical stress imparted by the internal pressure of a taut granule, we performed control experiments using cells in which vesicles were shrunken with hyperosmotic solutions. With these flaccid granules, again, the capacitance rise always preceded the swelling of the granules. We conclude that swelling cannot be the driving force for membrane fusion in this system.**

Even though membrane fusion is widely studied and is known to control a large set of cellular secretory processes, there is still little idea whether the membrane contact and continuity that define fusion precede or follow the mechanical disruptions that are morphologically seen as exocytosis. As is well recognized, when membrane continuity is established, the capacitance of the cell membrane increases (1). In a number of systems, granular swelling is clearly associated with exocytosis and exocytosis is clearly inhibited by hyperosmotic solutions (2, 3); these indirect experiments support the hypothesis that osmotic swelling is the driving force for exocytosis. However, in the digitonin-treated chromaffin cell, Holz and Senter showed that shrunken vesicles undergo exocytosis (4). If osmotic swelling drives membrane fusion, then swelling must precede fusion.

In the beige mouse, peritoneal mast cells typically have a few (1–10) large (2–6 μm in diameter) degranulating secretory granules (5, 6). This cell allows the detection of minute granular swelling by quantitative light microscopy, and the small number of granules allows us to correlate capacitive changes with individual secretory events. In this study we have combined patch clamp observation of cell membrane capacitance with video-enhanced microscopic observation of granular swelling to show that electrical events characteristic of fusion clearly *precede* the granular swelling that develops into the secretion of granular contents in mast cells of beige mice.

MATERIALS AND METHODS

Cell Isolation. Beige mice (C57BL/6N-*bg*) were obtained from the National Institutes of Health animal facility (7). Animals were sacrificed by cervical dislocation, and cells were obtained by peritoneal lavage with 150 mM NaCl/5 mM KCl/1 mM $CaCl_2$/2 mM $MgCl_2$/5.6 mM glucose/10 mM Hepes, pH 7.2. Cells were layered on cover slips, allowed to settle, and covered with a modified Eagle's medium (without bicarbonate) containing 10 mM Hepes, pH 7.2, and 62 mg of penicillin and 135 mg of streptomycin per liter.

Optical Measurements. Cells were viewed at room temperature with a Zeiss IM 435 inverted microscope with a 1.4 n.a. objective and a 0.63 n.a. long working distance condenser, differential interference optics, and deSénarmont compensation. Final magnification to the video screen was ×13,400. Due to the contrast sensitivity of video, the two-point limit of resolution of our system was ≈0.18 μm (8). [This limit is determined by the ability to separate two overlapping diffraction patterns. On the other hand, detecting a change in diameter depends upon defining the position of the peak of the diffraction pattern or, in the case of differential interference contrast, the position at which the contrast reverses. Thus, the ability to detect position change in an edge or line could be 5 or even much greater than the two-point resolution limit (S. Inoué, personal communication)]. Empirically, we could detect diameter increases of 0.084 μm, and we could therefore detect small changes in granular diameter during swelling (1.4–4.2%). When granules swell, the membrane sometimes separates from the internal matrix; in this case we could measure a membrane–matrix separation of 0.18 μm.

Electrical Measurements. A thin-walled, hard-glass, Sylgard-coated, 2- to 4-MΩ patch pipette was filled with an intracellular solution of 150 mM monopotassium glutamate/6 mM $MgCl_2$/0.1 mM EGTA/10 mM Hepes, pH 7.2/0.5 mM inosine triphosphate (ITP)/2–5 μM guanosine 5′-[3-thio]-triphosphate (GTP[γS]). We used a pipette solution based on that of Fernandez *et al.* (9) which utilizes GTP[γS] to induce fusion. We found that as the GTP[γS] concentration was increased from 2 μM to 10 μM, the interval between establishing whole-cell voltage clamp (i.e., internal perfusion) and the first secretory event became smaller, decreasing from on the order of minutes to tens of seconds. The extracellular solution was 140 mM NaCl/5 mM KCl/6 mM $CaCl_2$/1 mM $MgCl_2$/5.6 mM glucose/10 mM Hepes, pH 7.2. For experiments requiring hypertonic solutions, external and internal solutions were brought to 660 mosmol/kg with sucrose as determined with a vapor pressure osmometer

The publication costs of this article were defrayed in part by page charge payment. This article must therefore be hereby marked "*advertisement*" in accordance with 18 U.S.C. §1734 solely to indicate this fact.

Abbreviations: GTP[γS], guanosine 5′-[3-thio]triphosphate; ITP, inosine triphosphate.

*To whom reprint requests should be addressed.

(Wescor, Salt Lake City, UT). Tight-seal whole-cell recordings were obtained by standard techniques (10), and simultaneous capacitance and conductance measurements were made by the quadrature technique of Neher and Marty (11). A sine wave of 806 Hz and 20 mV or 100 mV peak-to-peak amplitude was applied across the membrane via a patch clamp (List EPC-7) in voltage clamp mode. The current output was applied to a two-channel lock-in amplifier (Ortholoc 9502). The phase was determined and a calibration pulse applied (11). The in-phase and out-of-phase signals were filtered by an 8-pole Bessel low-pass filter at a corner frequency of 200 Hz.

Synchronization of Electrical and Optical Measurements. At the beginning of each video field the capacitance and conductance outputs were sampled, converted into digital data, and displayed in the bottom of the same video field. The image of the granule was scanned by the video camera some 1–9 ms after the electrical measurements were sampled, depending upon the position of the granule on the video screen. A field-by-field (60 fields per s) display of capacitance, conductance, and time was superimposed upon the image of the secreting cell (see Fig. 1*a*). In addition, an image of the AC-coupled oscilloscope traces (50 ms per sweep) showing the capacitance and current was inserted onto the video field. Synchrony between the oscilloscope tracing and the video image could be determined to within a single video line (63.5 μs). For most experiments, the 1- to 9-ms digital/optical synchrony was adequate.

RESULTS

During exocytosis, surface area of the cell membrane increases when secretory granule membrane is added upon fusion. Because cell membrane capacitance is proportional to cell area, the moment of fusion should be marked by an increase in membrane capacitance. The large secretory granules of mast cells from beige mice allow capacitance measurements at wide bandwidth and the easy detection of granular swelling by light microscopy. To ensure close synchrony of the two measurements, we displayed the electrical record of capacitance next to the image of the granule, to directly compare changes in capacitance with changes in morphology.

Vesicle Fusion Precedes Granule Expansion in Isotonic Solution. We reproduced several sequential video fields documenting the increasing capacitance followed by granular swelling in Fig. 1. Whole-cell clamp was established, and the cell was perfused with the pipette medium containing 5 μM GTP[γS] and 0.5 mM ITP in order to induce fusion. ITP was

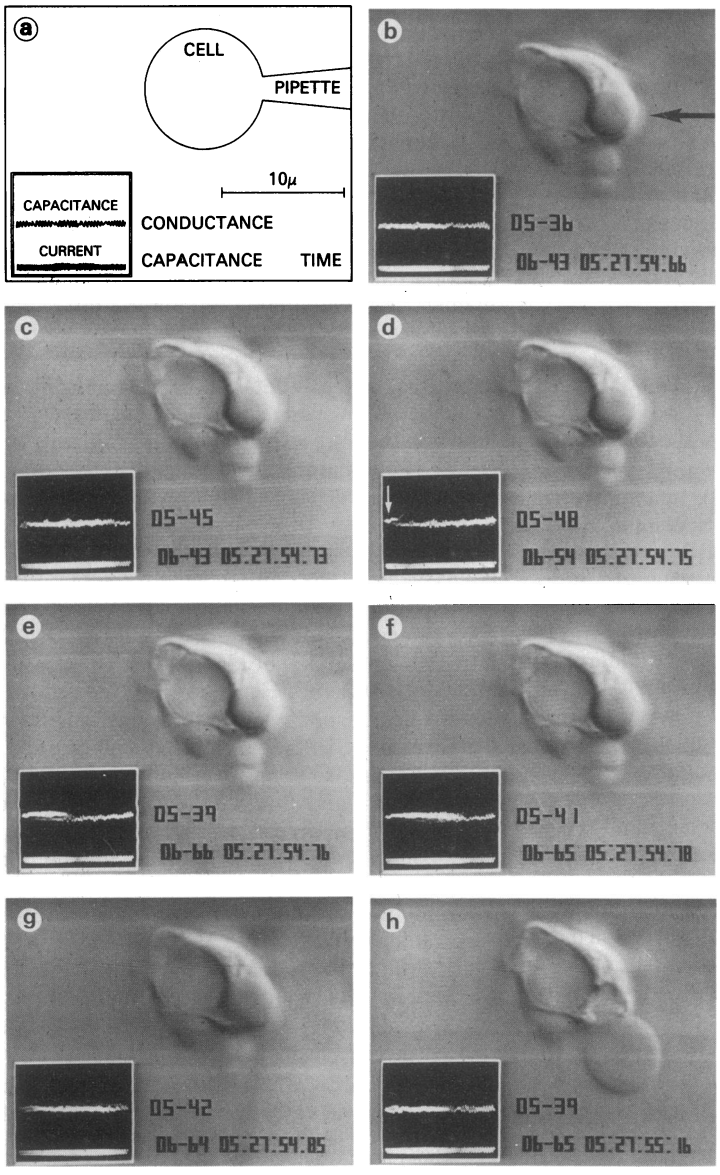

FIG. 1. The increase in capacitance occurs before granule swelling is detected. Fig. 1*a* is a key for the video fields that follow. From left to right, in the lower half of panels *b–h*, one sees the oscilloscope traces of capacitance and current, the four-digit readouts of conductance and capacitance, and the eight-digit timer with hr, min, s, and s $\times 10^{-2}$. Above is the cell image with the patch pipette located as in *a*; the image was taken with a Dage 65 video camera and stored on tape (Sony VO2850 U-matic video cassette recorder). Sequential frames of a typical experiment are shown. In *b* and *c* no activity occurs, but these fields provide a reference for granule size. The arrow points to the granule. In *d* capacitance changed from 643 to 654, and this jump is seen on the capacitance record of the oscilloscope tracing (arrow). In *e* the capacitance has risen to 666, but no granular swelling can be detected by morphometry. In the succeeding three fields (*f*, *g*, and *h*) swelling can be detected with no further change in capacitance. Conductance transiently changes during the experiment, but no average change corresponds with the fusion event. Capacitance calibration, 100 = 1 pF. Oscilloscope parameters: 50 ms/trace, persistence of 50 ms.

used rather than ATP to avoid increasing the permeability of the plasma membrane (12). Fig. 1*d* illustrates a jump in capacitance (arrow; ≈3 min after establishing whole-cell clamp) that continued for 17 ms (Fig. 1*e*). The granule did not appear to be swelling until 33 ms after capacitance had begun to increase (Fig. 1*f*). Fig. 1*h* chronicles the completion of the swelling in exocytosis. Capacitance remained constant during granule swelling and secretion of contents.

In 15 experiments (from eight cells), capacitance increases preceded granular swelling (Fig. 2). We rejected any experiments in which the granules were not in focus, ambiguity existed concerning assignment of identified granules, or large conductance changes accompanied the capacitance change. The interval between the initiation of capacitance increase and the initiation of granule swelling was 125 ± 23 ms (SEM, n = 15); the average time between exocytotic events was much longer, 48 ± 19 s. Thus we could correlate capacitance changes with morphological events. This correlation verified, on the single granule level, that the observed capacitance jumps were due to the fusion and the incorporation of granular membrane into plasma membrane. Further, the capacitance jumps typically increased over several video fields. The rise-times (half-maximal) of these increases ranged between 2 and 59 ms. Also, transient increases and decreases in capacitance of widely variable duration and amplitude, already reported in rat peritoneal mast cells (9), were also seen in beige mouse mast cells.

Fusion of Shrunken Granules in Hypertonic Media. It was possible that the granule membrane was already taut in the above experiments and that enough internal pressure existed within the granule to drive fusion without detectable swelling. For example, a 2–3% increase in area stretches lecithin membranes to cause rupture (1.5% change in diameter) (13). Curran (14) showed that granules in intact cells exposed to hypotonic solution reversibly swell, implying that granule membranes are flaccid in intact cells. However, granules in dialyzed cells that result from the whole-cell technique might behave differently. Cell-free granules, prepared by disrupting adherent mast cells with a rubber policeman (14), remained intact in 220 mosmol intracellular solution made hypotonic by the addition of distilled water, but the granules lysed at 200 mosmol. This would correspond to an 8% diameter increase for a spherical osmometer.

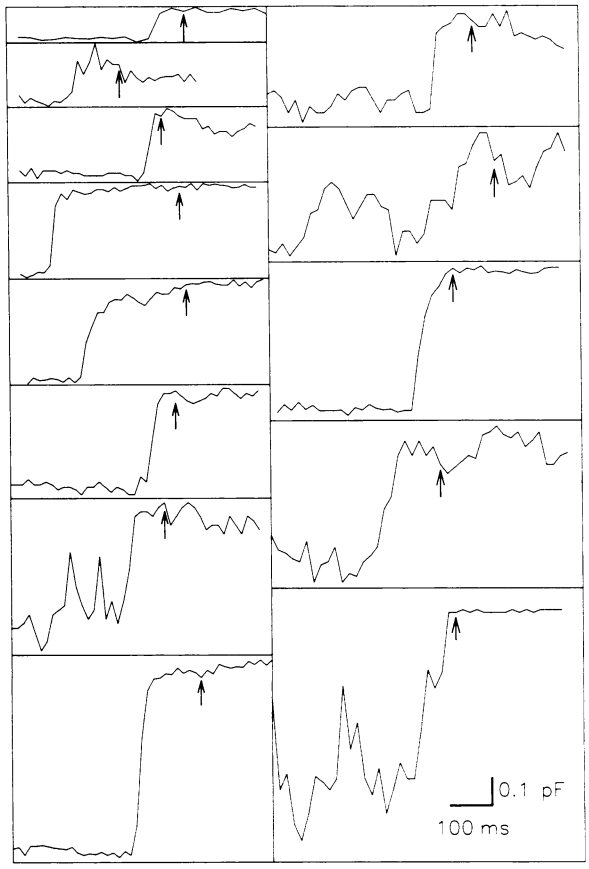

FIG. 2. Capacitance changes precede swelling in all experiments (isotonic milieu). Capacitance is shown as a function of time on the ordinate. Each box shows the record for one granule (13 granules in total), and the arrow marks time of detectable swelling. In all instances capacitance increase precedes swelling. Time and capacitance calibrations are identical for all records.

To further preclude the argument that the reason no swelling was observed before fusion was because the granule membrane was already taut, we treated cells with hyperosmotic sucrose solutions to see whether membrane fusion still preceded swelling. The shrinking of granules by treatment with hyperosmotic solution is shown in Fig. 3 [*a* in isotonic solution (280 mosmol) and *b* in hyperosmotic solution (660 mosmol)]. In a series of cells treated with this hyperosmotic milieu the average granule shrinkage, measured by reduction of the diameter, was 14 ± 2% (n = 5). Thirty-three minutes after treatment with hyperosmotic solutions, whole cell recording was initiated, and the cell was perfused with GTP[γS] and ITP to stimulate exocytosis (*c*); 104 s later (*d*), the first increase in capacitance was recorded, which continued for several fields (*d, e, f,* and *g*). The total change in capacitance was 0.26 pF. During the interval from the initiation of the whole cell mode to fusion, granule size was constant. After fusion capacitance remained constant for 5 s. Immediately after this interval—and not until then—swelling began (*h*), and exocytosis was soon complete (*i*). In four granule measurements in three cells, the capacitance increased before any detectable swelling occurred. The interval between these two events varied from 0.15 to 4.98 s. Thus, granules shrunken in hypertonic solution also fuse. Further, these granules, the membranes of which are presumably flaccid, do not swell before fusion.

To ensure that granules were indeed flaccid in these hyperosmotic patch clamp experiments, we subjected control cells to analogous osmolality changes and determined that the granules responded reversibly. We bathed cells for 33 min in hyperosmotic external medium, then for 1 min in hyperosmotic internal solution, and then disrupted the cells with a rubber policeman. We observed these granules with video microscopy while the hyperosmotic internal medium was replaced with the isotonic internal medium. The diameters of the granules increased by an average of 12.4 ± 1.7% (n = 9) without lysing. In our capacitance experiments, a 12.4% swelling of granules before fusion would have led to increases in diameter of 0.73, 0.55, 0.60, and 0.63 μm—well above the limit of detection for swelling (0.084 μm) and the detection limit for membrane-matrix separation (0.18 μm). Thus, the lack of swelling before the increases in capacitance demonstrates that flaccid vesicles had fused.

Specific Capacitance of Granule Membranes. The specific capacitance of biological membranes is typically on the order of 1 $\mu F/cm^2$ (1). Positive correlations between populations of granule surface area and capacitance changes associated with secretion have been made for rat mast cells (9). The small number and large size of the granules of the beige mouse mast cell allowed the correspondence of particular capacitance jumps with identified granules. A plot of measured capacitance increases versus calculated granule surface area (Fig. 4) gave a specific capacitance of 0.57 ± 0.05 $\mu F/cm^2$ in isotonic solutions and 0.58 ± 0.09 $\mu F/cm^2$ in hypertonic solutions. Although the estimate has several sources of error, the above value falls within the range reported for biological (1) and phospholipid membranes (15).

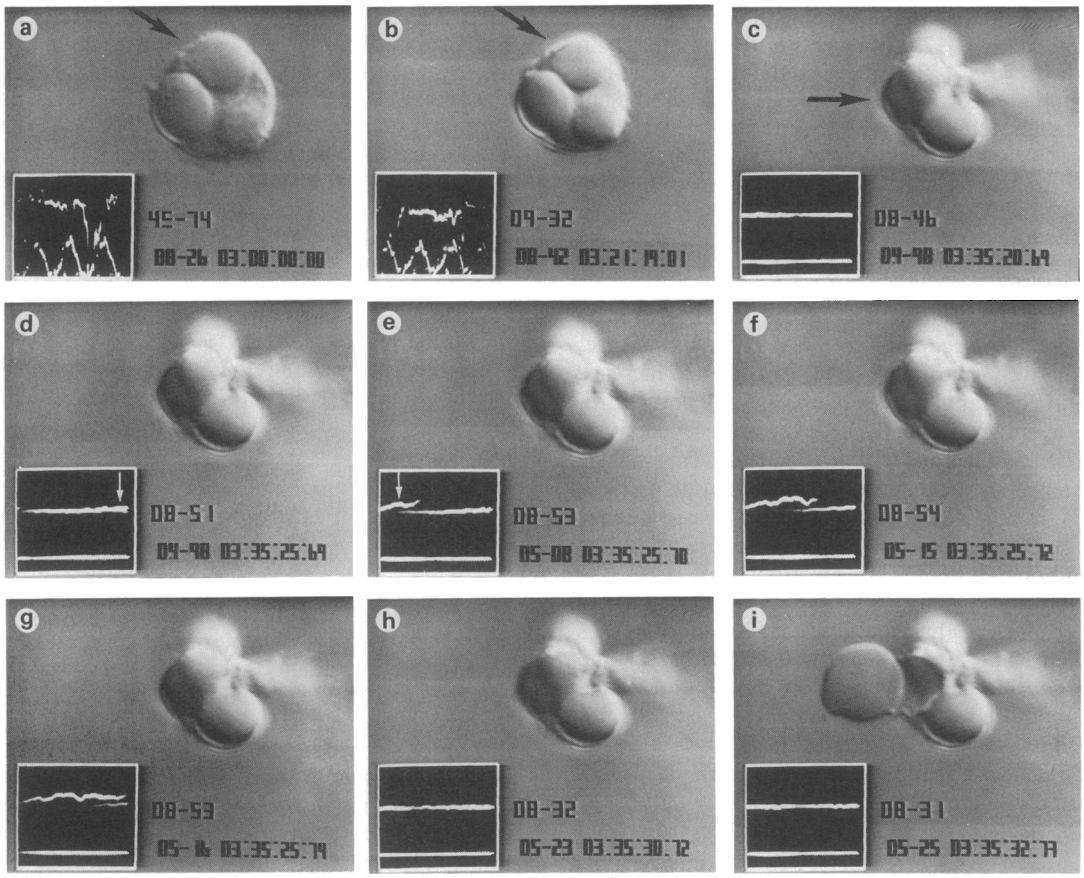

FIG. 3. Exocytosis of flaccid vesicles. In hyperosmotic solutions the cell membrane capacitance increases before granule swelling is detected. The oscilloscope tracings and digital readouts are configured as in Fig. 1*a*; (*a*) shows a mast cell with the topmost granule in focus (arrow). The cell is in the extracellular medium 140 mM NaCl/10 mM Hepes/6 mM $CaCl_2$/1 mM $MgCl_2$/5 mM KCl, pH 7.2. At time = 03:00:01:00 the solution was changed to extracellular medium plus 350 mM sucrose—final osmolality was 660 mosmol/kg. At 03:21:19:01 (*b*), the upper granule (arrow) is again in focus, and the vesicle had shrunk 12% in average diameter. The cell was rotated to allow for pipette sealing, and that upper granule is now the granule at left (arrow) in the fields after *b*. At 03:33:41:71 whole-cell recording and perfusion were begun. Ninety-nine seconds later *c* was recorded. In *d* (03:35:25:69; arrow), the first change in capacitance was detected and continues in *e*, *f*, and *g*. Swelling is not detected until 03:35:30:69, becomes clear in *h*, and is complete by *i*. Capacitance calibration: 85 = 1 pF.

DISCUSSION

We have combined high-resolution video microscopy and whole-cell capacitance measurements to examine exocytosis on the single granule level in mast cells of the beige mouse. These cells were used because (*i*) the large granule size permitted detection of swelling to within a 4.2% diameter increase, (*ii*) the large capacitance jumps allowed us to tolerate the increased noise that occurs with wide-bandwidth capacitance measurements, and (*iii*) the small number of granules per cell allowed the assignment of capacitance changes to identified granules.

To determine the role of osmotic forces in exocytosis we directly measured the temporal relationship between membrane fusion and vesicle swelling. If vesicle swelling produced taut membranes causing membrane fusion, swelling should precede fusion in flaccid vesicles. We found, however, that the capacitance increase associated with fusion *precedes any* detectable morphological changes. Increases in capacitance occurred before the mechanical events resulting in granule swelling began. *Therefore swelling cannot be the driving force for fusion in mast cells from beige mice.* In contrast, in vesicle-planar bilayer systems osmotic swelling of adherent vesicles is required for fusion (2, 16, 21). This requirement in the artificial system (which is *not* placed in doubt by the present study) led us to an osmotic hypothesis for biological fusion (2, 21). Based on other lines of evidence, investigators had previously proposed an osmotic hypothesis for fusion (2, 22, 23). Unless direct measurements in other systems show other results, we must accept this direct refutation of the osmotic hypothesis of exocytosis over many indirect experiments consistent with the hypothesis.

The reported capacitance increases associated with exocytosis were stable. In contrast, capacitance flickers (9)—increases followed by decreases—were frequently observed, but these flickers were never associated with swelling. We propose that such flickers result from the formation of an "exocytotic pore"—the lumen of the membrane neck that forms upon fusion connecting the interior of the granule with the extracellular space. As this pore enlarges and contracts, measured capacitance increases and decreases. We note that variable dilation of the exocytotic pore would result in nonquantal release of granule contents and capacitance flickers of sizes smaller than those sizes seen with exocytosis (9).

The increase in capacitance occurs over a range varying from the time resolution of our measurements (as fast as 3 ms) to tens of milliseconds, a time course we interpret to reflect the time course of widening of the exocytotic pore (Fig. 5). Before fusion the applied voltage drops solely across the cell membrane. After fusion the cell membrane is in parallel with the granule membrane. During exocytosis the applied voltage drops across the granule membrane and the exocytotic pore, which are in series. At the frequency of our applied sine wave, f = 806 Hz, the impedance of the granule membrane alone can be easily shown to be dominated by the granule capacitance, C_g, as opposed to the granule membrane resistance, R_g. Thus, when the pore resistance, R_p, is large

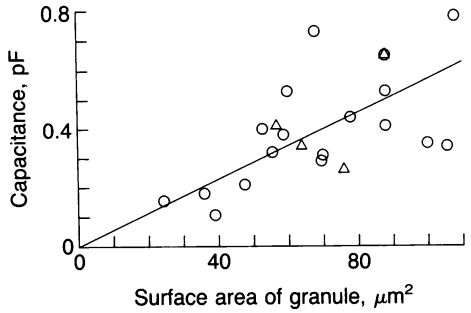

FIG. 4. Correlation of capacitance jump sizes with estimated granule surface area. Capacitance was measured as described, and granule surface area was determined before and after whole-cell perfusion; no difference in size was detected. To determine surface area, cells were visualized in differential interference contrast optics with very narrow depth of field to optically section the granules. A set of serial optical sections was made by focusing through the cell while recording images. The focal plane yielding the largest, most sharply focused granule cross-section was selected, and the perimeter of that granule cross-section traced off the video screen. The area of that tracing was measured with a digitizing tablet and hardware (Summagraphics, Fairfield, CT). That area was multiplied by four to yield the surface area of a sphere with an equivalent largest cross-sectional area. The linear regression line is shown. ○, Isotonic = 290 mosmol/kg; △, hypertonic = 660 mosmol/kg.

compared with the granule impedance, $1/(2\pi fC_g)$, the voltage drop is predominately across R_p, and there is little increase in the measured capacitance. As the pore dilates, pore resistance R_p decreases, the voltage drop across the granule membrane increases, and the detected capacitance increases. This apparent increase in capacitance is half-maximal value when $R_p = 1/(2\pi fC_g)$.

For different events we recorded times $t_{1/2}$ between the initiation of the capacitance growth and the half-maximal capacitance value over the range of 2–59 ms. From the measured capacitance jumps, we calculated that R_p was between 3.1×10^8 and 2.5×10^9 Ω at times = $t_{1/2}$. Assuming the pore to have the conductivity of bulk solution and a length of 100 Å, we estimate that at the time of half-maximal capacitance the pore diameter is between 18 and 52 Å. In *Limulus amoebocytes* the smallest exocytotic pore seen in freeze-substituted sections by electron microscopy was ≈100 Å wide and 150 Å long (17).

These estimates illustrate the utility of mast cells from beige mice for detailed studies of the time course of capacitance increases and flickers. Time course for the enlargement of this pore is best measured on cells with large granules. The large capacitance of these granules results in an improved signal-to-noise ratio, which allows faster (although noisier) measurements of cell capacitance. The larger granule capacitance results in smaller granule capacitative impedance, allowing a smaller R_p to develop before the full capacitance signal is measured.

Granule swelling may stabilize and widen the exocytotic pore. We found that a significant widening of this pore (i.e., the capacitance reaching its full value) preceded swelling. Movement of substances through the exocytotic pore and into the granule matrix may be responsible for swelling. If swelling is inhibited with hyperosmotic solutions, the transitory exocytotic pore may close or remain small, resulting in a kinetic inhibition of exocytosis (18). If R_p is large during hyperosmotic treatment, no capacitance change would be seen (19). The variation in both the time dependence and the osmotic pressure dependence of hyperosmotic inhibition as a function of molecular weight (4, 18, 19) suggests to us the possibility of a direct osmotic stress effect of the osmotic agents on the exocytotic pore (20).

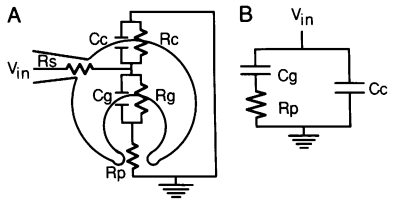

FIG. 5. (*A*) Sketch of the exocytotic pore that has resulted from fusion. Superimposed on the cartoon is the equivalent circuit. R_c and C_c, resistance and capacitance of the cell membrane; R_g and C_g, resistance and capacitance of the granule membrane; R_p, resistance of the exocytotic pore; and R_s, series resistance of the patch electrode. The phase of the lock-in amplifier was set as described (11), thereby compensating the phase shift induced by the series resistance. (*B*) The simplified equivalent circuit. R_c and R_g can be neglected for a sine wave of 806 Hz because $R_{c,g} << 1/2\pi fC_{c,g}$. The change in admittance as a result of fusion is given in complex notation by

$$\Delta Y(\omega) = R_p(\omega C_g)^2/((\omega C_g R_p)^2 + 1) + j(\omega C_g)/((\omega C_g R_p)^2 + 1).$$

Note that as a result of fusion, R_p varies from infinity, before fusion, to a small value after fusion. Fusion does not cause any net change in the real part of the admittance. But during the time that the capacitance increases, R_p decreases, and the real part of the admittance increases and then decreases. The maximum possible change (due to varying R_p) in the real component of the admittance equals $\omega C_g/2$, which is one-half the final change of the imaginary component, ωC_g. The experimental conductance transients (real component of the admittance) are in quantitative agreement with this theoretical prediction, lending support to this model.

We thank Rick Levis for an illuminating conversation on impedance measurements, Amy MacDermott, Naveh Moran, and Alain Marty for advice in setting up the patch clamp rig, Sandra York for advice and the use of video equipment, and V. Adrian Parsegian for support of this project. F.S.C. was supported by National Institutes of Health Grant GM27367.

1. Cole, K. S. (1968) *Membranes, Ions, and Impulses* (University of California, Berkeley, CA).
2. Finkelstein, A., Zimmerberg, J. & Cohen, F. S. (1986) *Annu. Rev. Physiol.* **48,** 163–174.
3. Holz, R. W. (1986) *Annu. Rev. Physiol.* **48,** 175–189.
4. Holz, R. W. & Senter, R. A. (1986) *J. Neurochem.* **46,** 1835–1842.
5. Poon, K. C., Liu, P. I. & Spicer, S. S. (1981) *Am. J. Pathol.* **104,** 142–149.
6. Chi, E. Y. & Lagunoff, D. (1975) *J. Histochem. Cytochem.* **23,** 117–122.
7. Lutzner, M. A., Lowrie, C. T. & Jordan, H. W. (1967) *J. Hered.* **58,** 299–300.
8. Inoué, S. (1986) *Video Microscopy* (Plenum, New York).
9. Fernandez, M., Neher, E. & Gomperts, B. D. (1984) *Nature (London)* **312,** 453–455.
10. Hamill, O. P., Marty, A., Neher, E., Sakmann, B. & Sigworth, F. J. (1981) *Pflügers Arch.* **391,** 85–100.
11. Neher, E. & Marty, A. (1982) *Proc. Natl. Acad. Sci. USA* **79,** 6712–6716.
12. Bennett, J. P., Cockcroft, S. & Gomperts, B. D. (1981) *J. Physiol. (London)* **317,** 335–345.
13. Kwok, R. & Evans, E. (1981) *Biophys. J.* **35,** 637–652.
14. Curran, M. J. (1986) Dissertation (University of Texas Medical Branch, Galveston, TX).
15. White, S. H. (1970) *Biophys. J.* **10,** 1127–1148.
16. Akabas, M. H., Cohen, F. S. & Finkelstein, A. (1984) *J. Cell Biol.* **98,** 1063–1071.
17. Ornberg, R. L. & Reese, T. S. (1981) *J. Cell Biol.* **90,** 40–54.
18. Zimmerberg, J., Sardet, C. & Epel, D. (1985) *J. Cell Biol.* **101,** 2398–2410.
19. Zimmerberg, J. & Whitaker, M. (1985) *Nature (London)* **315,** 581–584.
20. Zimmerberg, J. & Parsegian, V. A. (1986) *Nature (London)* **323,** 36–39.
21. Cohen, F. S., Zimmerberg, J. & Finkelstein, A. (1980) *J. Gen. Physiol.* **75,** 251–270.
22. Ferris, R. M., Viveros, O. H. & Kirshner, N. (1970) *Biochem. Pharmacol.* **19,** 505–514.
23. Pollard, H. B., Tack-Goldman, F., Pazoles, C. J., Creutz, C. E. & Shulman, N. R. (1977) *Proc. Natl. Acad. Sci. USA* **74,** 5295–5299.